



Published in final edited form as:

*Kidney Int.* 2010 July ; 78(2): 182–190. doi:10.1038/ki.2010.100.

## CYTOCHROME P450 2B1 GENE SILENCING ATTENUATES PUROMYCIN AMINONUCLEOSIDE-INDUCED CYTOTOXICITY TO GLOMERULAR EPITHELIAL CELLS

Niu Tian<sup>1</sup>, Istvan Arany<sup>1</sup>, David J. Waxman<sup>2</sup>, and Radhakrishna Baliga<sup>1</sup>

<sup>1</sup> Department of Pediatrics, University of Mississippi Medical Center, Jackson, MS 39216

<sup>2</sup> Department of Biology, Division of Cell and Molecular Biology, Boston University, Boston, MA 02215

### Abstract

Utilizing cytochrome P450 inhibitors we have recently demonstrated that P450 2B1 can serve as a site for reactive oxygen species generation in puromycin aminonucleoside (PAN)-induced nephrotic syndrome, which mimics minimal change disease in humans. In the current study, overexpression of P450 2B1 in glomerular epithelial cells significantly increased PAN-induced reactive oxygen species generation, cytotoxicity, cell death and collapse of the actin cytoskeleton. Silencing of P450 2B1 markedly attenuated reactive oxygen species generation, cytotoxicity, cell death and preserved the actin cytoskeleton. P450 2B1 protein content was significantly decreased while its mRNA level was markedly increased in the PAN-treated glomerular epithelial cells, indicating that the P450 2B1 protein decrease resulted from protein degradation rather than transcriptional inhibition. The degradation of P450 2B1 was accompanied by induction of heme oxygenase-1, an important indicator of heme-induced oxidative stress. This induction was significantly decreased in the P450 2B1-silenced cells treated with PAN. Treatment of the P450 2B1-silenced cells with PAN prevented cleavage of the endoplasmic reticulum-specific procaspase 12 and significantly decreased caspase 3 activity. Our data strongly suggests a pivotal role of P450 2B1 as an important site for reactive oxygen species production in PAN-induced cytotoxicity through an endoplasmic reticulum mediated pathway.

### Keywords

Cytochrome P450; Oxidative stress; Gene expression; Cytotoxicity

### INTRODUCTION

Reactive oxygen species (ROS) are important mediators of PAN induced experimental nephrotic syndrome, which mimics minimal change disease in humans<sup>1,2</sup>. The precise site and the source responsible for the generation of ROS are currently not well established. The cytochrome P450 (CYP) superfamily is a group of heme protein that act primarily as monooxygenases in the synthesis and metabolism of many endogenous and xenobiotic compounds<sup>3</sup>. However CYP can also function as oxidases and generate superoxide and

Address correspondence to: Radhakrishna Baliga, Research Wing R116A, 2500 North State Street, Jackson MS 39216; Phone: 601-984-5971; Fax: 601-815-5902; rbaliga@umsmed.edu.

### DISCLOSURE

All the authors declared no competing interests.

hydrogen peroxide ( $H_2O_2$ ) during the uncoupled oxidation of NADPH<sup>4-6</sup>. These ROS may cause breakdown of the CYP heme protein with the release of catalytic iron, which in turn generates more potent tissue damaging oxidants such as hydroxyl radical ( $OH\cdot$ ). The importance of CYP enzymes in the pathological processes of the kidney has become apparent during the past few years<sup>7-10</sup>. However the role of CYP as a site for ROS generation and a source of iron has not been fully explored. Moreover, the contribution of individual CYP enzymes to ROS generation leading to oxidative stress is only partially elucidated<sup>11-13</sup>. In our recent studies we have identified and localized CYP2B1 to the rat glomeruli and to glomerular epithelial cells (GEC) by Western blot and immunohistochemical analysis<sup>14,15</sup>. Generic CYP inhibitors markedly attenuated the PAN-induced proteinuria and cytotoxicity to the GEC<sup>14,15</sup>. The podocyte or GEC is a highly specialized cell and injury to these cells leads to the initiation and progression of nephrotic syndrome<sup>16,17</sup>. The major structural change in PAN-induced nephrotic syndrome is fusion of the foot processes of the GEC and focal detachment from the glomerular basement membrane<sup>18</sup>. The precise molecular mechanisms leading to this injury and proteinuria are poorly understood, although ROS have been implicated. We postulate that PAN, by interacting with CYP2B1 in the GEC, increases the formation of  $H_2O_2$ , which causes breakdown of the heme protein with the release of catalytic iron and heme. Catalytic iron promotes the generation of  $OH\cdot$  and other powerful oxidants causing injury. The released heme causes induction of heme oxygenase-1 (HO-1), which is protective<sup>19</sup>. The current study was designed to increase the specificity of our previous observations by ectopic expression of the CYP2B1 gene through adenovirus-mediated gene transfer and by knockdown of CYP2B1 using siRNA technology.

## RESULTS

### Overexpression/silencing of CYP2B1 in cultured GEC

We have previously identified and localized CYP2B1 to the GEC by immunocytochemistry and Western blot analysis<sup>14</sup>. In the current study, the expression of CYP2B1 mRNA in the cultured GEC was determined by real-time reverse transcriptase-polymerase chain reaction (RT-PCR). Both real time RT-PCR and western blot analysis indicated that the CYP2B1 has relatively low basal expression in the rat GEC. Hence all our current experiments were performed in GEC infected for 24 hr with an adenoviral vector that expresses rat CYP2B1 cDNA. Both real time RT-PCR and western blot analysis confirmed the expression of CYP2B1 (Fig. 1-A, B, C). A CYP2B1 siRNA mixture decreased both CYP2B1 mRNA and protein in GEC by ~ 65% after 48 hr transfection (Fig. 2-A, B, C).

### Overexpression of CYP2B1 exacerbates whereas silencing of CYP2B1 attenuates PAN-induced $H_2O_2$ and $OH\cdot$ generation, cytotoxicity and cell death

GEC infected with CYP2B1 virus showed a significant increase of  $H_2O_2$  generation prior to PAN treatment (Fig. 3A). Incubation of GEC overexpressing CYP2B1 with PAN (2.5mM) resulted in a marked increase in  $H_2O_2$  generation in a time dependent fashion (Fig. 3B) with a significant production of  $OH\cdot$  (Fig. 4). The increased ROS was accompanied by a significant increase in PAN-induced cytotoxicity and cell death as measured by LDH release and Trypan blue exclusion (Fig. 5). Infection with an empty adenovirus did not change significantly PAN-mediated  $H_2O_2$  production, LDH release or cell survival compared to control cells incubated with PAN (Fig. 3B, Fig. 5) suggesting that the changes caused by CYP2B1 overexpression are CYP2B1 gene specific. Moreover, CYP2B1 silencing prevented the marked increase in PAN mediated  $H_2O_2$  generation (Fig. 6), reduced the  $OH\cdot$  formation (Fig. 4) and significantly attenuated cytotoxicity and cell death (Fig. 7A). Calcein AM/EthD-1 fluorescent staining confirmed the above results. In untreated cells the percentage of dead cells (red fluorescence) was < 1%. Treatment with PAN increased the

number of dead cells to 28%. Transfection of cells with scrambled (negative) siRNA did not significantly change PAN-induced cells death (23%) while CYP2B1 siRNA decreased it to 13 % (Fig. 7B).

### **PAN-mediated loss of CYP2B1 is a post-translational event**

The breakdown of CYP2B1 protein is crucial for the release of catalytic iron and the formation of OH· resulting in injury. The CYP2B1 protein level was significantly decreased 1 hr after treatment of cultured GEC with PAN. In contrast, CYP2B1 mRNA levels measured at the same time were increased rather than decreased following PAN treatment (Fig. 8A, 8B). The increase in CYP2B1 mRNA may be due to compensation of the loss of CYP2B1 protein. These results suggest post-translational rather than transcriptional effects of PAN on the loss of CYP2B1 protein.

### **Induction of HO-1 by PAN**

We postulate that the breakdown of the CYP2B1 heme protein by ROS results in the release of heme, which causes induction of the HO-1, an additional feature of oxidative stress. There was marked up-regulation of HO-1 in the PAN treated GEC, as indicated by Western blotting. GEC transfected with CYP2B1 siRNA and treated with PAN showed a significant decrease in HO-1 induction (Fig. 9).

### **ER-associated caspase 12 activation**

Caspase 12 is an ER-specific caspase that plays a crucial role in the ER stress-induced apoptotic pathway<sup>20</sup>. CYP2B1 is an ER resident hemeprotein. Hence it was important to determine whether the oxidative stress resulting from the breakdown of CYP2B1 resulted in activation of the ER-specific caspase 12. In current study, pro-caspase 12 was significantly decreased in GEC treated with PAN for 48 hr while the active form of caspase 12 was increased. Cleavage of procaspase 12 was prevented in GECs transfected with CYP2B1 siRNA (Fig. 10A). Similarly, caspase 3 activity was markedly increased in the GEC treated with PAN and this was significantly attenuated in the CYP2B1 siRNA transfected cells (Fig. 10B).

### **Effect of CYP2B1 gene silencing on PAN induced reorganization of actin filament**

The actin cytoskeletal structure plays an important role in maintaining the architecture of the podocyte foot processes<sup>21</sup>. We therefore examined the effect of CYP2B1 gene silencing on the morphological changes of GEC treated with PAN. Prior to PAN treatment, F-actin staining revealed a characteristic spindle-like appearance of the GEC with numerous cell processes and prominent actin stress fibers. Treatment of the GEC with PAN resulted in retraction of the processes with disruption of the actin filaments (Fig. 11). CYP2B1 gene silencing protected the cells from PAN-induced actin reorganization, whereas the scrambled siRNA did not show any protective effects. These results suggest that PAN-induced disruption of the actin cytoskeleton is mediated through CYP2B1.

## **DISCUSSION**

CYP enzymes are not only crucial in the elimination of foreign compounds but also play a pivotal role in the generation of ROS that are associated with cell damage<sup>22</sup>. We have identified and localized CYP2B1 to rat GEC. CYP2B1 is expressed at a very low basal level in primary hepatocytes<sup>23</sup> and in GEC, as shown by real time RT-PCR and western blot analysis. In cultured rat hepatocytes, phenobarbital induction of CYP2B1 is most pronounced<sup>24,25</sup>. However, we have not been able to demonstrate increased induction of CYP2B1 in phenobarbital-treated kidney glomeruli and GEC (data not shown), consistent

with the observations of Guengerich et al <sup>13,26</sup>. Hence our experiments in the current study were performed in GEC infected with an adenoviral vector that encodes the rat CYP2B1 cDNA.

ROS play an important role in the alteration of the GEC morphology leading to proteinuria <sup>27,28</sup>. Utilizing CYP inhibitors we have demonstrated marked reduction in ROS generation with attenuation of proteinuria in a PAN model of nephrotic syndrome and PAN-induced GEC cytotoxicity <sup>14,15</sup>. The current study extends those findings by gene-specific targeting of CYP2B1. Both *in vivo* and *in vitro* studies have shown that CYP2B1 induction by Phenobarbital (PB) treatment was selectively associated with oxidative stress <sup>29,30</sup>. Recent studies indicated that the ability of phenobarbital to selectively induce *in vivo* oxidative stress was related to decreases in glutathione peroxidase and pyridine nucleotides, which normally protect cells from ROS <sup>13,26</sup>. In the current study, ROS generation in GEC overexpressing CYP2B1 was significantly higher than in control cells even in the basal state (Fig. 3A.). Moreover, exposure of these CYP2B1 overexpressing cells to PAN markedly increased ROS generation and significantly increased cytotoxicity. These results suggest that the changes resulting from CYP2B1 overexpression are gene specific (Fig. 3A, B and Fig. 5). Silencing of CYP2B1 attenuated PAN-induced ROS generation and cytotoxicity. Therefore, CYP2B1 is indeed the source of generation of intracellular H<sub>2</sub>O<sub>2</sub> leading to oxidant injury.

The heme moiety of the CYP may serve as an important source of catalytic iron capable of catalyzing free radical reactions <sup>9,31-34</sup>. CYP inactivation in the PAN-treated cells may involve the formation of active oxygen species accompanied by bleaching of the heme protein as a result of heme loss or degradation <sup>35</sup>. The CYP would then be inactivated and catabolized with the release of heme and catalytic iron, which promotes the generation of OH· and induces lipid peroxidation. In the present study the marked increase in OH· generation in PAN-treated GEC was significantly decreased upon silencing of CYP2B1 (Fig. 4), confirming the role of CYP2B1 in the generation of the OH· and subsequent injury.

The induction of CYP2B1 mRNA by phenobarbital can be modulated in a redox sensitive manner <sup>22</sup>. Redox regulation of CYP2B1 mRNA in GEC is also suggested in the present study, where CYP2B1 mRNA levels were increased 4-fold within 1 h of PAN treatment, at which time CYP2B1 protein was significantly decreased (Fig. 8). This increase in CYP2B1 mRNA may be a compensatory effect to replace the CYP2B1 protein. Furthermore, these results indicate a post-translational rather than a post-transcriptional effect of PAN on the loss of CYP2B1 protein.

Agents that promote the induction of the heme-degrading enzyme HO-1 cause a release of the heme from CYP, which in turn leads to activation of HO-1 <sup>36</sup>. HO-1 was induced in PAN-treated glomeruli and GEC following marked generation of H<sub>2</sub>O<sub>2</sub> and degradation of CYP2B1, which was attenuated by CYP inhibitors <sup>14,15</sup>. In our current study HO-1 induction was markedly increased in PAN-treated GECs with a significant decrease in the CYP2B1-silenced cells (Fig. 9). Thus, breakdown of the CYP2B1 heme protein leads to the release of heme, which in turn induces HO-1. A similar protective effect was observed following stabilization of CYP by carbon monoxide, thus preventing its degradation, induction of HO-1 and oxidative stress <sup>10</sup>.

Caspases are cysteine proteases that play an important role in programmed cell death <sup>37,38</sup>. Fogo et al have shown a marked increase in the active form of caspase 3 in PAN-induced apoptosis <sup>39</sup>. Caspase 3 activity was markedly increased following PAN treatment but was significantly decreased in the CYP2B1-silenced cells (Fig. 10B). Caspase 12 is an ER-specific caspase that participates in apoptosis under ER stress <sup>20,40,41</sup>. It is an initiator

caspace that undergoes activation in response to apoptotic stimuli and in turn activates downstream effector caspases that are responsible for the cleavage of a wide variety of physiologic substrates<sup>42</sup>. The PAN-induced increase in the active form of caspase 12 was significantly ameliorated in the GEC transfected with CYP2B1 siRNA (Fig. 10A). Caspase 12 and caspase 3 could be functioning in conjunction with each other or independently.

Actin cytoskeleton is a major constituent of the glomerular foot processes and reorganization of the actin filaments leads to effacement of the foot processes<sup>17</sup>. There is increasing evidence to indicate that PAN induces actin cytoskeletal depolarization that can result in structural changes of the podocyte and leakage of the protein through the slit diaphragm<sup>43-46</sup>. CYP inhibitors enhance the preservation of individual foot processes of the podocytes and protect from PAN-induced proteinuria<sup>15</sup>. In the current study CYP2B1 gene silencing prevented the disruption of the actin cytoskeleton induced by PAN (Fig. 11), confirming that the disorganization of the actin cytoskeleton is mediated by CYP2B1 induced oxidative stress in an *in vitro* model of PAN-induced cytotoxicity.

Experimental animal models are commonly utilized to predict the mechanism of podocyte injury in the humans despite species variability<sup>47</sup>. Majority of the rat strains are prone to PAN induced injury with effacement of foot processes and development of proteinuria while most of the mice strains have been traditionally resistant<sup>48,49</sup>. Differences in the genetic traits including prior presence of hypercholesterolemia have been associated to the development of PAN induced proteinuria<sup>50-52</sup>. Harris et al. have shown that PAN induces reversible proteinuric injury in transgenic mice expressing COX-2 in the podocytes<sup>53</sup>. Expression of COX-2 in the vascular endothelial cells has been linked to the CYP<sup>54</sup>. Prostanoids have also been shown to down regulate PB induced CYP 2B1 gene expression<sup>55</sup>. There are marked specific inter and intra tissue differences in the expression and inducibility of the CYP in the different strains and species<sup>56</sup>. This may determine the generation of H<sub>2</sub>O<sub>2</sub>, breakdown of the heme protein, release of catalytic iron and the formation of the hydroxyl radical leading to disruption of the cytoskeleton and proteinuria based on the interaction between PAN and CYP2B1. We have not been able to demonstrate the expression of the CYP2B1 in the 129/SV strain of mice glomeruli both by immunohistochemistry and western blot analysis ( unpublished data ). Transgenic mice with expression of CYP2B1 in the podocyte may provide better understanding of the pathogenesis of PAN induced nephrotic syndrome. Autophagy represents an important protective mechanism that attempts to rescue cells from apoptosis<sup>57,58</sup>. In a recent communication Huber et al observed significant level of autophagy in the podocytes in mice under pathophysiological conditions and this loss of autophagy resulted in increased susceptibility to injury in models of glomerular disease (Renal Week 2009, San Diego, CA, F-FC 275).

In conclusion, utilizing CYP2B1 gene specific silencing we have confirmed that CYP2B1 plays a crucial role as the primary site for the generation of ROS. Furthermore, we have shown that PAN acts at the level of CYP2B1 protein to increase production of ROS and induce degradation of CYP2B1 protein with the release of heme and iron. The free iron participates in the OH· generation while the heme causes induction of HO-1. The resultant cytotoxicity and cell death is mediated through an ER stress-associated apoptotic pathway. These findings may facilitate the identification of specific CYP forms in human kidney that exert functions similar to CYP2B1 and thus offer a valuable therapeutic target in the treatment of minimal change disease in humans.

## MATERIALS AND METHODS

### Cell culture

Rat GEC (kindly provided by Dr. S. Kasinath, University of Texas Health Science Center) were maintained in DMEM/F12 (1:1) medium supplemented with 10% of fetal bovine serum, 100 units/ml of insulin, 5% penicillin/streptomycin in a humidified atmosphere of 5% CO<sub>2</sub>-95% air at 37°C and fed at intervals of 3 days as described<sup>14</sup>.

### Adenoviral infection

GEC grown in 6-well-plates were incubated in full medium containing 1×10<sup>8</sup> IFU/ml adenovirus vector that contains the rat CYP2B1 gene<sup>59</sup> for 3 hr at 37°C. The cells were then washed with culture medium and further incubated in full medium for 24 hr at 37°C. Empty adenovirus (AdNull, Vector Biolabs) was used as a negative control.

### CYP2B1 gene silencing

The experiments were performed in 6-well plates in triplicate when cells reached 60%–70% confluence, according to the manufacturer's recommendation (Dharmacon). In brief, transfection reagent (DharmaFECT #1, 6 µl per well) and rat CYP2B1 siRNA (ON-TARGET plus SMART pool L-081876-01-0010) solution (20nM) were prepared. These two components were mixed and added to antibiotic-free complete medium and the cells incubated for 48 hr at 5% CO<sub>2</sub>-95% air at 37°C. The extent of knockdown was determined by real-time RT-PCR and Western blotting.

### Measurement of intracellular H<sub>2</sub>O<sub>2</sub> generation in GEC

The intracellular generation of H<sub>2</sub>O<sub>2</sub> in GEC was assayed using the oxidant-sensitive fluorescent dye dichlorodihydrofluorescein diacetate (DCFDA)<sup>60</sup>. In brief, confluent GEC were cultured in the presence or absence of adenovirus, harvested by trypsinization and suspended in DPBS buffer. Cell suspensions were then transferred into a microplate (2–5×10<sup>5</sup> cells/well) and incubated at room temperature with DCFDA (10 µg/ml) with or without PAN (2.5 mM) for 30 min. At the end of the incubation, the fluorescence intensity of cell suspension was read up to 150 min using a fluorescence plate reader (excitation at 485nm, emission at 535 nm).

### Measurement of OH<sup>•</sup> production

2-Deoxy-D-ribose in a final concentration of 3 mM was added to the medium just prior to the incubation with or without PAN (2.5 mM). At the end of 150 min incubation, the incubation medium was collected for the measurement of OH<sup>•</sup> formation by deoxyribose degradation method<sup>61</sup>.

### Measurement of cytotoxicity

Cytotoxicity was assessed by the “CytoTox-One Homogenous Membrane Integrity” assay kit (Promega, Madison, WI, U.S.A.). After 48 hr treatment with or without 2.5 mM PAN an aliquot of the growth medium was removed and saved. The monolayer was lysed according to the manufacturer's recommendation and LDH content was determined by a colorimetric substrate both in the medium and cell lysate. LDH release was calculated as a percentage of LDH content in the medium compared to the total LDH content (medium+lysate)<sup>62</sup>.

### Cell viability/survival

Viable cell count was determined by trypan blue (Sigma, St. Louis, MO) exclusion using a hemocytometer. To determine the extent of cell viability the “LIVE/DEAD Viability/



Cytotoxicity Assay kit” (Invitrogen) was used as suggested by the manufacturer. The kit contains two fluorescent dyes: calcein AM, which is retained by live cells and emits green fluorescence; and Ethidium-1 (EthD-1), which is taken up by damaged cells but excluded by live cells: it emits red fluorescence. Briefly, cells grown in 6-well-plates were treated with or without 2.5 mM PAN for 48 hr in the presence or absence of either a scrambled siRNA or a CYP2B1 siRNA. Monolayers were washed with PBS and stained with calcein AM and EthD-1 for 20 min. After repeated washing with PBS, red and green fluorescence was observed using a Nikon Eclipse TS100F inverted fluorescent microscope at 100× magnification. The % of dead cells was determined by counting dead (red) and live (green) cells.

### Western blotting

Monolayers of GEC were lysed in a radio-immunoprecipitation (RIPA) buffer that contained Protease inhibitor cocktail (Sigma-Aldrich). Protein content was determined by using a BioRad Protein Determination assay kit (BioRad Hercules, CA, U.S.A.) as described earlier<sup>63</sup>. In brief 100 µg of cell lysate protein was separated by SDS/PAGE electrophoresis and transferred to a PVDF membrane (BioRad, Hercules, CA, U.S.A.). The filters were hybridized with the appropriate primary antibodies followed by an HRP-conjugated secondary antibody. The bands were visualized by an ECL method (Pierce) and quantified by densitometry (UnScan-It Gel v6.1, Silk Scientific, Ore, UT, U.S.A.). Polyclonal goat anti-rat CYP2B1 antibody was obtained from Daiichi Pure Chemicals CO., LTD. Polyclonal anti-rat caspase-12 and anti-rat-HRP antibodies were purchased from Sigma-Aldrich (St. Louis, MO, U.S.A.). Anti-mouse actin antibody was purchased from Millipore. Anti-goat HRP-conjugated secondary antibody was purchased from Cell Signaling Technology (Santa Cruz, U.S.A.).

### Determination of caspase-3/7 activity

Caspase-3/7 activity was determined using the “Caspase-Glo® 3/7 Assay” kit (Promega) as recommended by the manufacturer. Briefly, GEC monolayers were treated with or without 2.5 mM PAN in the presence or absence of either a scrambled siRNA or a CYP2B1 siRNA. After 48 hr the Caspase-Glo® 3/7 reagent was added and incubated at room temperature for 30 min. Luminescence was determined in a Modulus Luminometer (Turner BioSystem).

### Real-time RT-PCR

Real-time RT-PCR assays were performed using iQ™ SYBR® Green Supermix (BioRad Laboratories) on an iCycler iQ™ Real-Time PCR Detection System (BioRad Laboratories). CYP2B1 primer was designed using the sequence obtained from rat CYP2B1 (Genbank accession J00719). Forward sequence: 5'-CGCATGGAGAAGGAGAAGTC-3' and reverse sequence: 5'-GCCGATCACCTGATCAATCT-3'. Relative fold change in mRNA level was quantified by using the 2- $\Delta\Delta C_t$  mathematical model<sup>64</sup>.

### Immunofluorescence

GEC grown on coverglass were transiently transfected with scrambled or CYP2B1-specific siRNAs as described above. After 48 hr the medium was replaced with fresh one that contained 2.5 mM PAN. After 48 hr PAN treatment the cells were washed with PBS and fixed in 4% paraformaldehyde for 10 min at room temperature followed by permeabilization with 0.1% Triton X-100 for 5 min at room temperature. The cells were washed, labeled with Alexafluor 488 phalloidin (Invitrogen) and counterstained with DAPI (Invitrogen) as recommended by the manufacturer. Fluorescence was observed using a Nikon Eclipse TS100F inverted microscope equipped with a FITC and CY3 filter at 400× magnification.

Images were captured by a Nikon DS cooled camera and analyzed with the NIS Elements Basic Research 3.0 software.

### Statistical analysis

Continuous variables were expressed as mean and standard deviation (S.D.). Means of multiple treatment groups were compared to controls by using of the Student's t-test. A *p*-value < 0.05 was considered statistically significant. All analyses were performed using a SigmaStat 3.5 software package.

### Acknowledgments

This study was partly supported by intramural research support program through the University of Mississippi Medical Center (RB), by an American Heart Association Midwest Affiliate Grant-in-Aid (0655716Z, IA) and by NIH grant 5 P42 ES07381, Superfund Research Program at Boston University (DJW). An abstract of this study was presented in part at the 2008 Annual Meeting of the American Society of Nephrology and at the 2009 Annual Meeting of the Pediatric Academic Societies.

### References

1. Ueda N, Baliga R, Shah SV. Role of 'catalytic' iron in an animal model of minimal change nephrotic syndrome. *Kidney Int* 1996;49:370–373. [PubMed: 8821819]
2. Gonick, H. *Current Nephrology*. Mosby Year Book; Chicago: 1997.
3. Nelson DR, Koymans L, Kamataki T, et al. P450 superfamily: update on new sequences, gene mapping, accession numbers and nomenclature. *Pharmacogenetics* 1996;6:1–42. [PubMed: 8845856]
4. Kuthan H, Tsuji H, Graf H, et al. Generation of superoxide anion as a source of hydrogen peroxide in a reconstituted monooxygenase system. *FEBS Lett* 1978;91:343–345. [PubMed: 210047]
5. Ekstrom G, Ingelman-Sundberg M. Rat liver microsomal NADPH-supported oxidase activity and lipid peroxidation dependent on ethanol-inducible cytochrome P-450 (P-450IIE1). *Biochem Pharmacol* 1989;38:1313–1319. [PubMed: 2495801]
6. Nordblom GD, Coon MJ. Hydrogen peroxide formation and stoichiometry of hydroxylation reactions catalyzed by highly purified liver microsomal cytochrome P-450. *Arch Biochem Biophys* 1977;180:343–347. [PubMed: 18091]
7. Hirt DL, Jacobson HR. Functional effects of cytochrome P450 arachidonate metabolites in the kidney. *Semin Nephrol* 1991;11:148–155. [PubMed: 1903553]
8. Carroll MA, Balazy M, Huang DD, et al. Cytochrome P450-derived renal HETEs: storage and release. *Kidney Int* 1997;51:1696–1702. [PubMed: 9186856]
9. Baliga R, Zhang Z, Baliga M, et al. Role of cytochrome P-450 as a source of catalytic iron in cisplatin-induced nephrotoxicity. *Kidney Int* 1998;54:1562–1569. [PubMed: 9844132]
10. Nakao A, Faleo G, Shimizu H, et al. Ex vivo carbon monoxide prevents cytochrome P450 degradation and ischemia/reperfusion injury of kidney grafts. *Kidney Int* 2008;74:1009–1016. [PubMed: 18633343]
11. Liu L, Bridges RJ, Eyer CL. Effect of cytochrome P450 1A induction on oxidative damage in rat brain. *Mol Cell Biochem* 2001;223:89–94. [PubMed: 11681726]
12. Isayama F, Froh M, Bradford BU, et al. The CYP inhibitor 1-aminobenzotriazole does not prevent oxidative stress associated with alcohol-induced liver injury in rats and mice. *Free Radic Biol Med* 2003;35:1568–1581. [PubMed: 14680680]
13. Dostalek M, Brooks JD, Hardy KD, et al. In vivo oxidative damage in rats is associated with barbiturate response but not other cytochrome P450 inducers. *Mol Pharmacol* 2007;72:1419–1424. [PubMed: 17898314]
14. Liu H, Baliga M, Bigler SA, et al. Role of cytochrome P450 2B1 in puromycin aminonucleoside-induced cytotoxicity to glomerular epithelial cells. *Nephron Exp Nephrol* 2003;94:e17–e24. [PubMed: 12806184]



15. Liu H, Bigler SA, Henegar JR, et al. Cytochrome P450 2B1 mediates oxidant injury in puromycin-induced nephrotic syndrome. *Kidney Int* 2002;62:868–876. [PubMed: 12164868]
16. Shankland SJ. The podocyte's response to injury: role in proteinuria and glomerulosclerosis. *Kidney Int* 2006;69:2131–2147. [PubMed: 16688120]
17. Mundel P, Shankland SJ. Podocyte biology and response to injury. *J Am Soc Nephrol* 2002;13:3005–3015. [PubMed: 12444221]
18. Caulfield JP, Reid JJ, Farquhar MG. Alterations of the glomerular epithelium in acute aminonucleoside nephrosis. Evidence for formation of occluding junctions and epithelial cell detachment. *Lab Invest* 1976;34:43–59. [PubMed: 1246124]
19. Dennery PA. Regulation and role of heme oxygenase in oxidative injury. *Curr Top Cell Regul* 2000;36:181–199. [PubMed: 10842752]
20. Liu H, Baliga R. Endoplasmic reticulum stress-associated caspase 12 mediates cisplatin-induced LLC-PK1 cell apoptosis. *J Am Soc Nephrol* 2005;16:1985–1992. [PubMed: 15901768]
21. Lachapelle M, Bendayan M. Contractile proteins in podocytes: immunocytochemical localization of actin and alpha-actinin in normal and nephrotic rat kidneys. *Virchows Arch B Cell Pathol Incl Mol Pathol* 1991;60:105–111. [PubMed: 1675506]
22. Hirsch-Ernst KI, Schlaefer K, Bauer D, et al. Repression of phenobarbital-dependent CYP2B1 mRNA induction by reactive oxygen species in primary rat hepatocyte cultures. *Mol Pharmacol* 2001;59:1402–1409. [PubMed: 11353799]
23. Lee CM, Kim BY, Li L, et al. Nitric oxide-dependent proteasomal degradation of cytochrome P450 2B proteins. *J Biol Chem* 2008;283:889–898. [PubMed: 17993647]
24. Waxman DJ, Azaroff L. Phenobarbital induction of cytochrome P-450 gene expression. *Biochem J* 1992;281 ( Pt 3):577–592. [PubMed: 1536639]
25. Honkakoski P, Negishi M. Protein serine/threonine phosphatase inhibitors suppress phenobarbital-induced Cyp2b10 gene transcription in mouse primary hepatocytes. *Biochem J* 1998;330 ( Pt 2): 889–895. [PubMed: 9480906]
26. Dostalek M, Hardy KD, Milne GL, et al. Development of oxidative stress by cytochrome P450 induction in rodents is selective for barbiturates and related to loss of pyridine nucleotide-dependent protective systems. *J Biol Chem* 2008;283:17147–17157. [PubMed: 18442974]
27. Kawaguchi M, Yamada M, Wada H, et al. Roles of active oxygen species in glomerular epithelial cell injury in vitro caused by puromycin aminonucleoside. *Toxicology* 1992;72:329–340. [PubMed: 1585386]
28. Ricardo SD, Bertram JF, Ryan GB. Reactive oxygen species in puromycin aminonucleoside nephrosis: in vitro studies. *Kidney Int* 1994;45:1057–1069. [PubMed: 8007575]
29. Imaoka S, Osada M, Minamiyama Y, et al. Role of phenobarbital-inducible cytochrome P450s as a source of active oxygen species in DNA-oxidation. *Cancer Lett* 2004;203:117–125. [PubMed: 14732219]
30. Tong V, Chang TK, Chen J, et al. The effect of valproic acid on hepatic and plasma levels of 15-F2t-isoprostane in rats. *Free Radic Biol Med* 2003;34:1435–1446. [PubMed: 12757854]
31. Baliga R, Zhang Z, Baliga M, et al. Evidence for cytochrome P-450 as a source of catalytic iron in myoglobinuric acute renal failure. *Kidney Int* 1996;49:362–369. [PubMed: 8821818]
32. Bysani GK, Kennedy TP, Ky N, et al. Role of cytochrome P-450 in reperfusion injury of the rabbit lung. *J Clin Invest* 1990;86:1434–1441. [PubMed: 2173718]
33. Paller MS, Jacob HS. Cytochrome P-450 mediates tissue-damaging hydroxyl radical formation during reoxygenation of the kidney. *Proc Natl Acad Sci US A* 1994;91:7002–7006.
34. Liu H, Shah SV, Baliga R. Cytochrome P-450 as a source of catalytic iron in minimal change nephrotic syndrome in rats. *Am J Physiol Renal Physiol* 2001;280:F88–F94. [PubMed: 11133518]
35. Karuzina II, Archakov AI. Hydrogen peroxide-mediated inactivation of microsomal cytochrome P450 during monooxygenase reactions. *Free Radic Biol Med* 1994;17:557–567. [PubMed: 7867972]
36. Bissell DM, Hammaker LE. Cytochrome P-450 heme and the regulation of hepatic heme oxygenase activity. *Arch Biochem Biophys* 1976;176:91–102. [PubMed: 970967]

37. Howley B, Fearnhead HO. Caspases as therapeutic targets. *J Cell Mol Med* 2008;12:1502–1516. [PubMed: 18298652]
38. Degtarev A, Boyce M, Yuan J. A decade of caspases. *Oncogene* 2003;22:8543–8567. [PubMed: 14634618]
39. Kanjanabuch T, Ma LJ, Chen J, et al. PPAR-gamma agonist protects podocytes from injury. *Kidney Int* 2007;71:1232–1239. [PubMed: 17457378]
40. Yoneda T, Imaizumi K, Oono K, et al. Activation of caspase-12, an endoplasmic reticulum (ER) resident caspase, through tumor necrosis factor receptor-associated factor 2-dependent mechanism in response to the ER stress. *J Biol Chem* 2001;276:13935–13940. [PubMed: 11278723]
41. Rao RV, Peel A, Logvinova A, et al. Coupling endoplasmic reticulum stress to the cell death program: role of the ER chaperone GRP78. *FEBS Lett* 2002;514:122–128. [PubMed: 11943137]
42. Morishima N, Nakanishi K, Takenouchi H, et al. An endoplasmic reticulum stress-specific caspase cascade in apoptosis. Cytochrome c-independent activation of caspase-9 by caspase-12. *J Biol Chem* 2002;277:34287–34294. [PubMed: 12097332]
43. Eto N, Wada T, Inagi R, et al. Podocyte protection by darbepoetin: preservation of the cytoskeleton and nephrin expression. *Kidney Int* 2007;72:455–463. [PubMed: 17457371]
44. Ransom RF, Lam NG, Hallett MA, et al. Glucocorticoids protect and enhance recovery of cultured murine podocytes via actin filament stabilization. *Kidney Int* 2005;68:2473–2483. [PubMed: 16316324]
45. Koshikawa M, Mukoyama M, Mori K, et al. Role of p38 mitogen-activated protein kinase activation in podocyte injury and proteinuria in experimental nephrotic syndrome. *J Am Soc Nephrol* 2005;16:2690–2701. [PubMed: 15987752]
46. Shibata S, Nagase M, Fujita T. Fluvastatin ameliorates podocyte injury in proteinuric rats via modulation of excessive Rho signaling. *J Am Soc Nephrol* 2006;17:754–764. [PubMed: 16452496]
47. Brosius FC III, Alpers CE, Bottinger EP, et al. Mouse models of diabetic nephropathy. *J Am Soc Nephrol* 2009;20:2503–2512. [PubMed: 19729434]
48. Fogo AB. Animal models of FSGS: lessons for pathogenesis and treatment. *Semin Nephrol* 2003;23:161–171. [PubMed: 12704576]
49. Pippin JW, Brinkkoetter PT, Cormack-Aboud FC, et al. Inducible rodent models of acquired podocyte diseases. *Am J Physiol Renal Physiol* 2009;296:F213–F229. [PubMed: 18784259]
50. Cheng ZZ, Patari A, Aalto-Setälä K, et al. Hypercholesterolemia is a prerequisite for puromycin inducible damage in mouse kidney. *Kidney Int* 2003;63:107–112. [PubMed: 12472773]
51. Zheng Z, Pavlidis P, Chua S, et al. An ancestral haplotype defines susceptibility to doxorubicin nephropathy in the laboratory mouse. *J Am Soc Nephrol* 2006;17:1796–1800. [PubMed: 16775033]
52. Chen A, Wei CH, Sheu LF, et al. Induction of proteinuria by adriamycin or bovine serum albumin in the mouse. *Nephron* 1995;69:293–300. [PubMed: 7753263]
53. Jo YI, Cheng H, Wang S, et al. Puromycin induces reversible proteinuric injury in transgenic mice expressing cyclooxygenase-2 in podocytes. *Nephron Exp Nephrol* 2007;107:e87–e94. [PubMed: 17890881]
54. Michaelis UR, Falck JR, Schmidt R, et al. Cytochrome P450C9-derived epoxyeicosatrienoic acids induce the expression of cyclooxygenase-2 in endothelial cells. *Arterioscler Thromb Vasc Biol* 2005;25:321–326. [PubMed: 15569819]
55. Li CC, Lii CK, Liu KL, et al. n-6 and n-3 polyunsaturated fatty acids down-regulate cytochrome P-450 2B1 gene expression induced by phenobarbital in primary rat hepatocytes. *J Nutr Biochem* 2006;17:707–715. [PubMed: 16517146]
56. Bogaards JJ, Bertrand M, Jackson P, et al. Determining the best animal model for human cytochrome P450 activities: a comparison of mouse, rat, rabbit, dog, micropig, monkey and man. *Xenobiotica* 2000;30:1131–1152. [PubMed: 11307970]
57. Lemasters JJ, Nieminen AL, Qian T, et al. The mitochondrial permeability transition in cell death: a common mechanism in necrosis, apoptosis and autophagy. *Biochim Biophys Acta* 1998;1366:177–196. [PubMed: 9714796]

58. Elmore S. Apoptosis: a review of programmed cell death. *Toxicol Pathol* 2007;35:495–516. [PubMed: 17562483]
59. Tzanakakis ES, Waxman DJ, Hansen LK, et al. Long-term enhancement of cytochrome P450 2B1/2 expression in rat hepatocyte spheroids through adenovirus-mediated gene transfer. *Cell Biol Toxicol* 2002;18:13–27. [PubMed: 11991083]
60. Rosenkranz AR, Schmaldienst S, Stuhlmeier KM, et al. A microplate assay for the detection of oxidative products using 2',7'-dichlorofluorescein-diacetate. *J Immunol Methods* 1992;156:39–45. [PubMed: 1431161]
61. Baliga R, Zhang Z, Shah SV. Role of cytochrome P-450 in hydrogen peroxide-induced cytotoxicity to LLC-PK1 cells. *Kidney Int* 1996;50:1118–1124. [PubMed: 8887268]
62. Quigg RJ, Cybulsky AV, Jacobs JB, et al. Anti-Fx1A produces complement-dependent cytotoxicity of glomerular epithelial cells. *Kidney Int* 1988;34:43–52. [PubMed: 3172636]
63. Bradd SJ, Dunn MJ. Analysis of membrane proteins by western blotting and enhanced chemiluminescence. *Methods Mol Biol* 1993;19:211–218. [PubMed: 7693221]
64. Livak KJ, Schmittgen TD. Analysis of relative gene expression data using real-time quantitative PCR and the 2(-Delta Delta C(T)) Method. *Methods* 2001;25:402–408. [PubMed: 11846609]

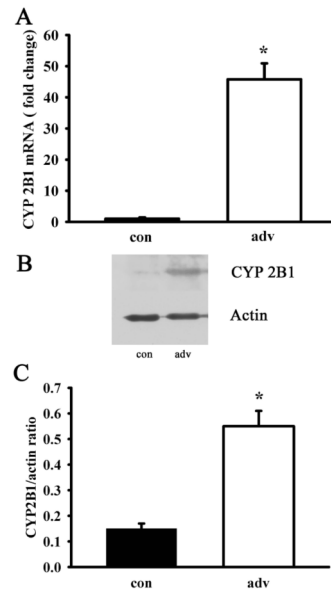


**Fig. 1. Upregulation of CYP2B1 mRNA and protein by adenovirus in GEC**

(A) CYP2B1 mRNA levels were detected by real-time RT-PCR in GEC 24 hr after infecting with a CYP2B1 adenovirus (adv) as described in Methods. (B) Protein levels of CYP2B1 were determined by Western blotting in GEC 24 hr after infecting with a CYP2B1 adenovirus (adv). The blots are representatives of three independent experiments. (C) Densitometric analysis of the blots are shown. Values are mean  $\pm$  SE, \* $p$ <0.05, compared to untreated or control (con) GEC.

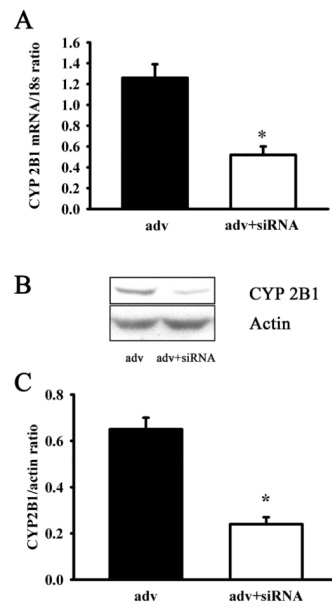


**Fig. 2. siRNA-mediated knockdown of CYP2B1 mRNA and protein in GEC**

(A) CYP2B1 mRNA levels were detected in GEC that overexpress the CYP2B1 gene (adv) and transiently transfected with the CYP2B1 siRNA mixture for 48 hr by real-time RT-PCR. (B) Protein levels of the CYP2B1 were determined in the GEC treated as in (A) by Western blotting. The blots shown are representatives of three independent experiments. (C) Densitometric analysis of the blots are shown. Values are mean  $\pm$  SE, \* $p < 0.05$  compared to adv.

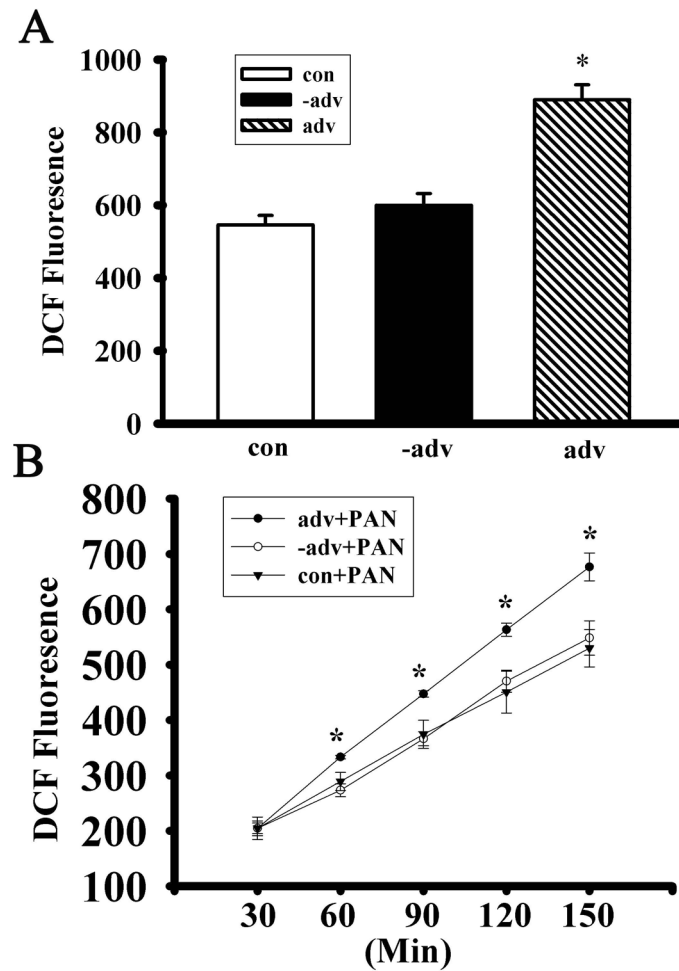


**Fig. 3. Generation of  $H_2O_2$  in the GEC that overexpress the CYP2B1 gene in the basal state and following addition of PAN**

(A) Generation of  $H_2O_2$  was determined in the GEC infected with the CYP2B1 expressing adenovirus (adv) or an empty adenovirus (-adv) and control (con) cells in the basal state prior to the addition of PAN. (B) Generation of  $H_2O_2$  was measured in the GEC infected with the CYP2B1 expressing adenovirus (adv) or an empty adenovirus (-adv) and control (con) cells between 30 and 150 min following treatment with or without 2.5mM PAN by the oxidant-sensitive fluorescent dye DCFH-DA. Data at each time point represents net  $H_2O_2$  production ( PAN induced minus respective control) and are mean  $\pm$ SE, n=3, \*p<0.05 compared to con cells treated with PAN.



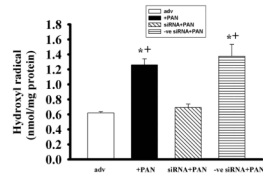


**Fig. 4. Effect of CYP2B1 siRNA on hydroxyl radical formation in GEC treated with PAN**  
 CYP2B1 gene was silenced (siRNA) in GEC infected with the CYP2B1 expressing adenovirus (adv) and treated with or without 2.5 mM PAN. Generation of hydroxyl radical was determined at 150 min following treatment with PAN. To demonstrate the specificity of CYP2B1 siRNA, a negative siRNA (–ve siRNA) group was included. Values are mean  $\pm$  SE, n=3, \*p<0.05, compared to adv cells; + p<0.05, compared to siRNA+PAN.

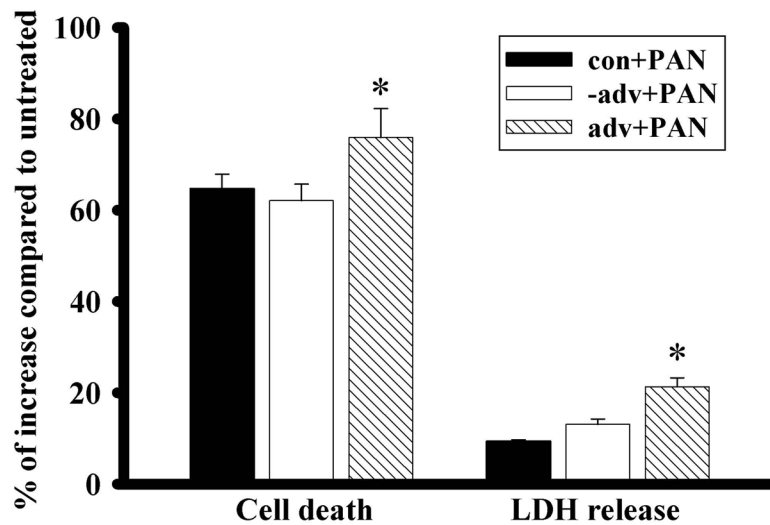


**Fig. 5. Effect of overexpression of CYP2B1 on cytotoxicity and cell death in GEC**  
Cytotoxicity (LDH release) and cell viability (trypan blue exclusion) were determined in the control (con) cells and in the GEC infected with a CYP2B1 (adv) or a negative adenovirus (-adv) following 48 hr treatment with or without 2.5 mM PAN. Data represents percentage of increase compared to respective untreated control. Values are mean  $\pm$  SE, n=3, \*p<0.05, compared to con+PAN.

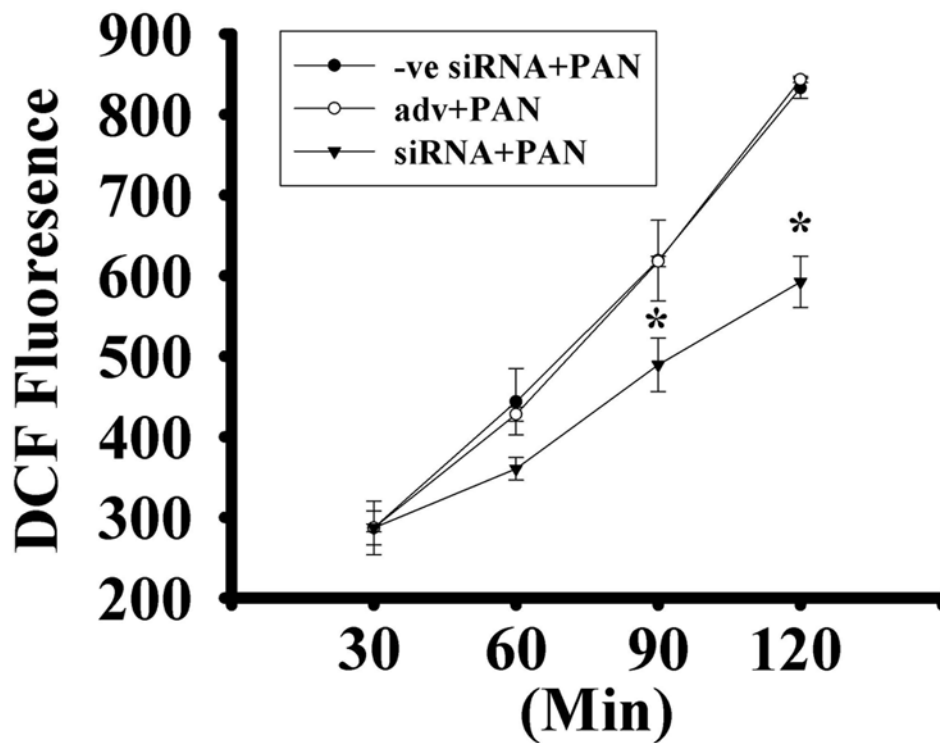


**Fig. 6. Effect of CYP2B1 siRNA on PAN-induced generation of  $H_2O_2$  in GEC**  
CYP2B1 gene was silenced in GEC infected with CYP2B1 adenovirus (adv) and treated with or without 2.5 mM PAN. Intracellular generation of  $H_2O_2$  was measured by the oxidant sensitive fluorescent dye DCFH-DA 30 to 120 min following treatment with PAN. A negative siRNA group was included to increase the specificity of our observation. Data at each time point represent net  $H_2O_2$  production (PAN-induced less its own endogenous control). Values are mean  $\pm$  SE,  $n=3$ , \* $p<0.05$  compared to adv+PAN

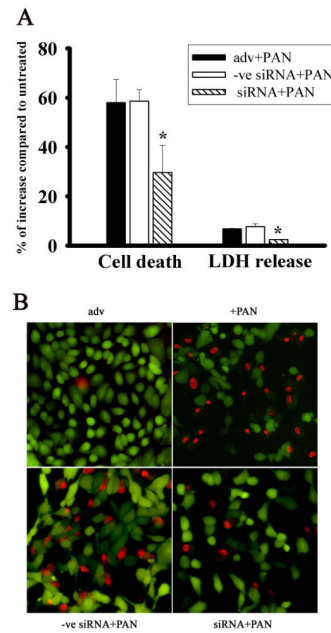


**Fig. 7. Effect of CYP2B1 siRNA on PAN-induced cytotoxicity and cell death in GEC**  
**(A)** GEC were infected with CYP2B1 expressing adenovirus (adv) and treated with or without 2.5 mM PAN. LDH release and trypan blue exclusion were determined 48 hr after treatment in GEC that were non transfected and transiently transfected with CYP2B1 siRNA or negative siRNA and expressed as percentage of untreated controls. Values are mean  $\pm$  SE, n=3, \*p<0.05 compared to adv+PAN. **(B)** Presence of live (green fluorescence) and dead (red fluorescence) cells were determined in GEC infected with CYP2B1 expressing adenovirus (adv) 48 hr following treatment with or without 2.5 mM PAN in the presence of CYP2B1 siRNA or negative siRNA as described in Methods. Picture shown is representative of three independent experiments.

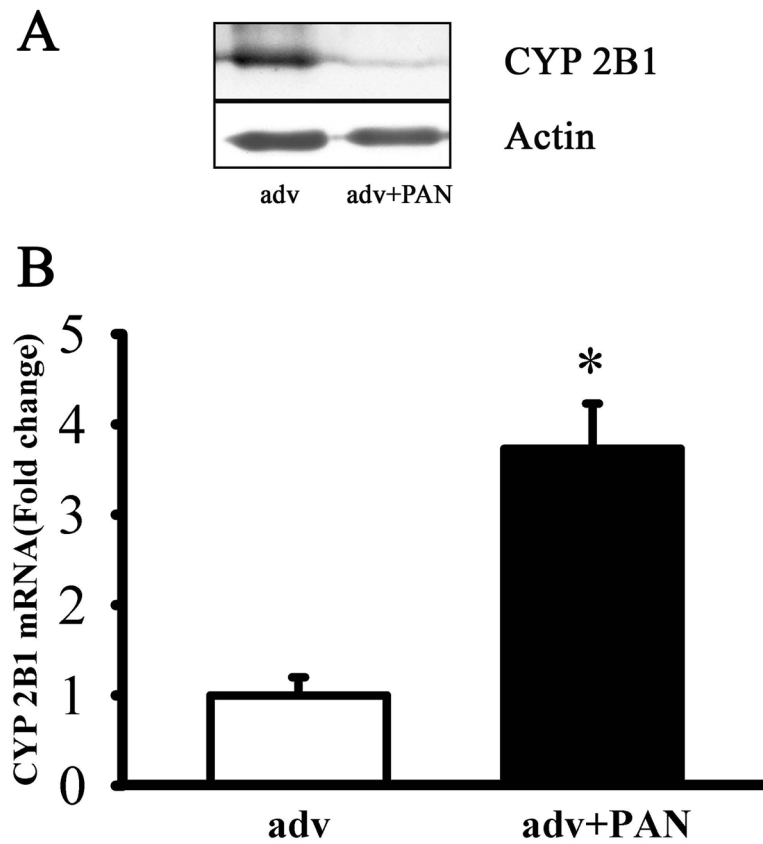


**Fig. 8. Effect of PAN treatment on mRNA and protein levels of CYP2B1 in GEC**  
(A) Protein levels of CYP2B1 were determined by Western blotting in CYP2B1 overexpressing GEC (adv) following incubation with or without 2.5 mM PAN for 1hr. The blots shown are representatives from three independent experiments. (B) Similarly, CYP2B1 mRNA levels were detected by real-time RT-PCR in GEC overexpressing the CYP2B1 gene 1 hr after incubation with or without 2.5 mM PAN. Values are  $\pm$  SE,  $n=3$ ,  $*p<0.05$  compared to adv.

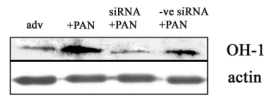


**Fig. 9. Effect of knockdown of CYP2B1 gene on HO-1 level following treatment with PAN**  
Level of HO-1 protein was determined by Western blotting in the CYP2B1 overexpressing GEC (adv) following 48 hr treatment with or without 2.5 mM PAN in the presence of CYP2B1 siRNA or negative siRNA. The blots shown are a representation of three independent experiments.



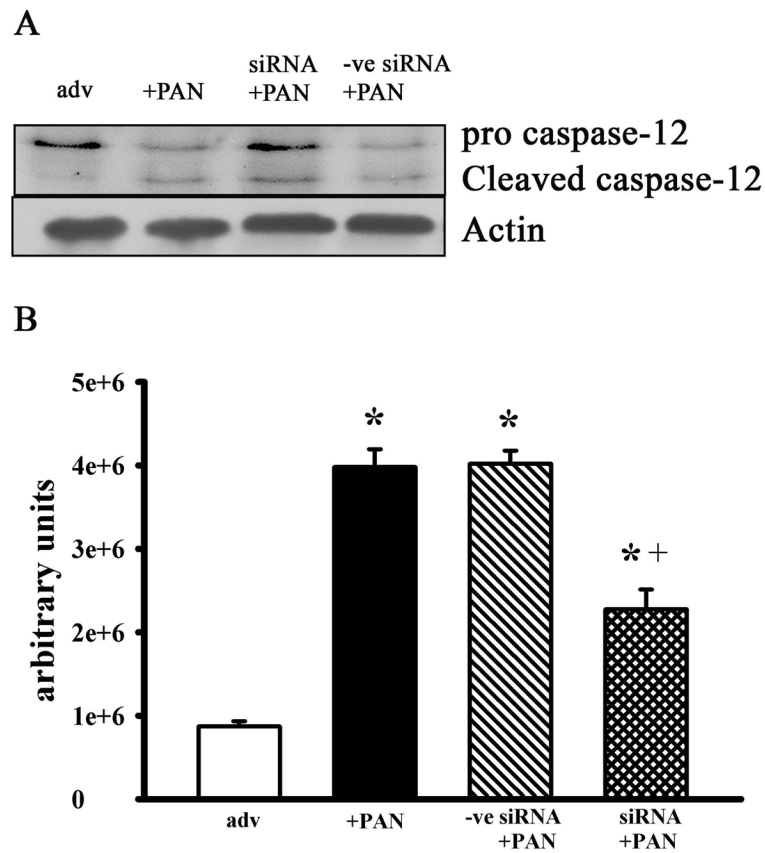


**Fig. 10. Effect of PAN treatment on caspase-12 cleavage and caspase-3 activity in GEC**  
**(A)** Pro and cleaved caspase 12 were determined by Western blotting in the CYP2B1 overexpressing GEC (adv) at 48 hr after treatment with or without 2.5 mM PAN in the presence of CYP2B1 siRNA or negative siRNA. The blots shown are Representation of three independent experiments. **(B)** Caspase 3 activity was measured in the GEC treated as in (A) 48 hr following incubation with or without 2.5 mM PAN in the presence of CYP2B1 siRNA or negative siRNA as described in methods. Values represent arbitrary units of luminescence and are mean  $\pm$  SE, \* $p < 0.001$ , compared to adv, + $p < 0.001$  compared to +PAN..

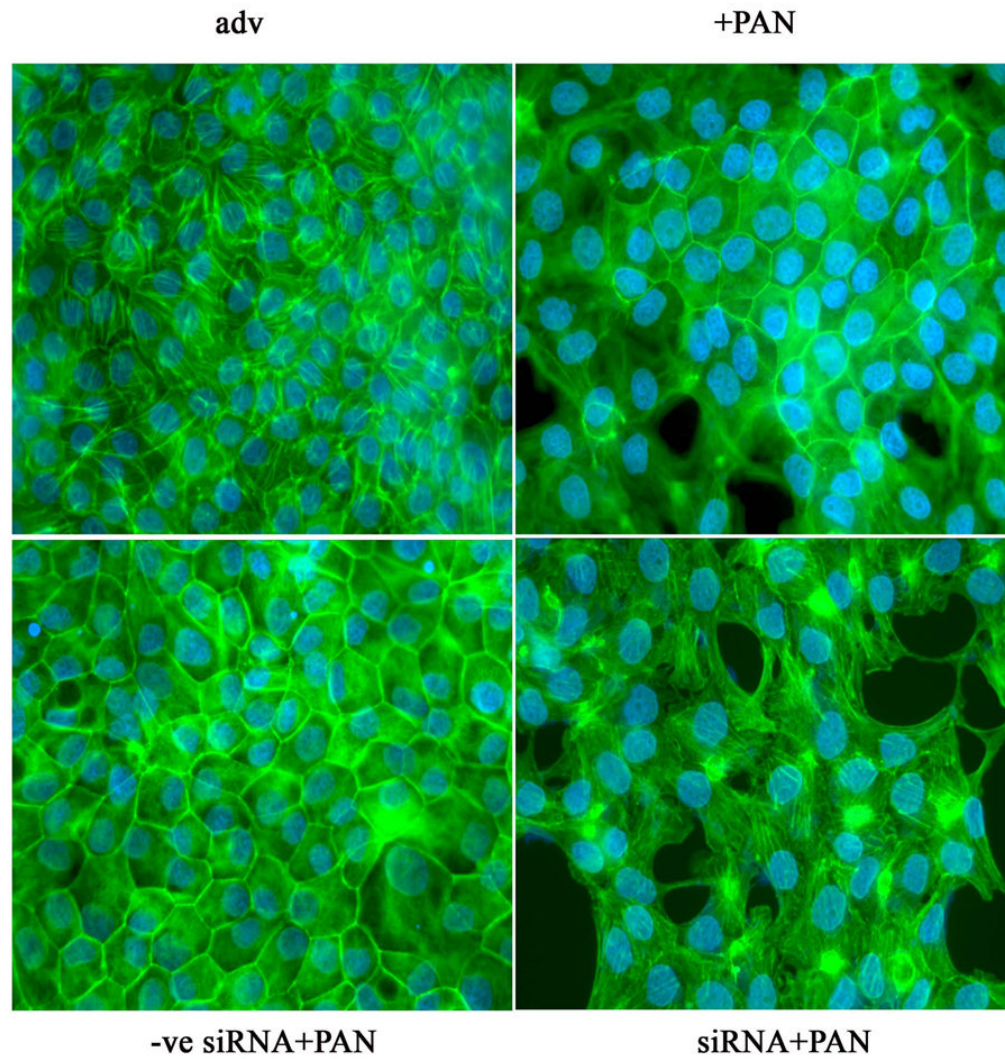


**Fig. 11. Effect of CYP2B1 gene silencing on PAN-induced reorganization of the actin cytoskeleton**

CYP2B1 overexpressing GEC (adv) were treated with or without 2.5 mM PAN for 48 hr in the presence of CYP2B1 siRNA or negative siRNA. Cells were fixed, permeabilized and hybridized with an Alexaflour 488-conjugated phalloidin as described in Methods. Pictures are representative of three independent experiments.